In vivo Effects of Vaccination with Six-Transmembrane Epithelial Antigen of the Prostate: A Candidate Antigen for Treating Prostate Cancer

Maria de la Luz Garcia-Hernandez,[1] Andrew Gray,[1] Bolyn Hubby,[2] and W. Martin Kast[1]

[1]Department of Molecular Microbiology and Immunology, Norris Comprehensive Cancer Center, Los Angeles, California and
[2]AlphaVax, Inc., Research Triangle Park, North Carolina

Abstract

Immunotherapy may provide an alternative treatment for cancer patients, especially when tumors overexpress antigens that can be recognized by immune cells. The identification of markers and therapeutic targets that are up-regulated in prostate cancer has been important to design new potential treatments for prostate cancer. Among them, the recently identified six-transmembrane epithelial antigen of the prostate (STEAP) is considered attractive due to its overexpression in human prostate cancer tissues. Our study constitutes the first assessment of the *in vivo* effectiveness of STEAP-based vaccination in prophylactic and therapeutic mouse models. Two delivery systems, cDNA delivered by gene gun and Venezuelan equine encephalitis virus-like replicon particles (VRP), both encoding mouse STEAP (mSTEAP) and three vaccination strategies were used. Our results show that mSTEAP-based vaccination was able to induce a specific CD8 T-cell response against a newly defined mSTEAP epitope that prolonged the overall survival rate in tumor-challenged mice very significantly. This was achieved without any development of autoimmunity. Surprisingly, CD4 T cells that produced IFNγ, tumor necrosis factor-α (TNF-α), and interleukin-2 (IL-2) played the main role in tumor rejection in our model as shown by using CD4- and CD8-deficient mice. In addition, the presence of high IL-12 levels in the tumor environment was associated with a favorable antitumor response. Finally, the therapeutic effect of STEAP vaccination was also assessed and induced a modest but significant delay in growth of established, 31 day old tumors. Taken together, our data suggest that vaccination against mSTEAP is a viable option to delay tumor growth. [Cancer Res 2007;67(3):1344–51]

Introduction

Prostate cancer is the most commonly diagnosed malignancy in the western world and is the second leading cause of cancer-related death in American males (1). Patients who develop recurrent disease after surgical prostate excision or radiation therapy may be treated with androgen deprivation strategies, but the effectiveness of this treatment lasts <18 months on average, when most patients develop hormone-refractory prostate cancer (HRPC; ref. 2). The median survival in patients with HRPC is ~12 months (3). Chemotherapy is effective in the treatment of prostate cancer, although long-term chemotherapy is not feasible due to its intrinsic toxicity (4). Currently, the therapeutic options are very limited for advanced cases, particularly in patients with metastatic tumors. Immunotherapy is a promising and specific prospective treatment for localized and metastatic disease.

The immunotherapeutic treatments to date have involved the use of antigen-presenting cells (APC) that are loaded with specific peptides or are modified by transduction or transfection. These cells are crucial for presenting antigen to CD8 T cells, which are critical to the host defense against malignancies (5). Most immunotherapy strategies specifically target overexpressed prostate cancer–associated self-antigens, such as prostate-specific antigen (PSA; ref. 6), prostate stem cell antigen (7), prostate-specific membrane antigen (8), and prostatic acid phosphatase (9). The majority of current clinical trials have failed to induce effective tumor immune responses that can reduce patient tumor burden. Recently, six-transmembrane epithelial antigen of the prostate (STEAP) was identified in advanced human prostate cancer. Biochemical and secondary structure analyses suggested that this protein could function as a channel, receptor, or transporter protein; however, its function is currently unknown. Under physiologic conditions, low levels of STEAP have been detected in plasma membranes of normal prostate tissues but it is highly overexpressed in human prostate cancer tissue. STEAP has also been detected in several colon, bladder, ovarian, and pancreatic cancer cell lines, reinforcing the idea that this gene may be generally up-regulated in transformed cells (10). We identified recently the murine counterpart of human STEAP (hSTEAP), expressed in a prostate tumor cell line (TRAMPC-2) derived from the prostate of mice of the transgenic adenocarcinoma mouse prostate (TRAMP) model. Analysis of the nucleotide and amino acid sequences of mouse STEAP (mSTEAP) showed 80% homology with hSTEAP and that it also contains six potential membrane-spanning regions. In TRAMP mice, mSTEAP is expressed at high levels in malignant prostate tissue (11).

Central and peripheral tolerance inhibit the induction of immune responses to self-antigens, such as STEAP. Central tolerance leads to deletion of T cells that express high-avidity T-cell receptors (TCR) specific for self-antigens. Low numbers of these T cells in the periphery may be responsible for the ineffective antitumor T-cell responses observed in cancer patients. Recently, hSTEAP peptides were identified as excellent inducers of antigen-specific CTL that were able to recognize and kill STEAP-expressing tumor cells (12) and stimulate specific $CD8^+$ T cells from HLA-A*0201 healthy donors (13). These data suggest that STEAP is a potential candidate antigen for prostate cancer immunotherapy.

Successful immunotherapy strategies must be based on systems that enhance expression or cross-presentation of self-peptides to naive T cells in secondary lymphoid tissues. One of the most

Note: Supplementary data for this article are available at Cancer Research Online (http://cancerres.aacrjournals.org/).

Requests for reprints: W. Martin Kast, University of Southern California, 1501 San Pablo Street, ZNI 245, Los Angeles, CA 90033. Phone: 323-442-3870; Fax: 323-442-4433; E-mail: mkast@usc.edu.

doi:10.1158/0008-5472.CAN-06-2996

successful treatments is a heterologous prime-boost vaccination regime, involving sequential vaccination using different antigen delivery systems encoding the same antigen. DNA prime/virus boost regimes are the most commonly used to increase immunogenicity (14). A viral vector system, in which vaccine-related genes are expressed by an attenuated strain of the Venezuelan equine encephalitis (VEE) virus, can elicit potent cellular immune responses and protective immunity against implanted tumors (15). This system has many advantages, including high level of expression of heterologous genes and vector amplification through double-stranded RNA intermediates, which avoids integration of genetic material into the host DNA. In addition, it stimulates innate immunity, through activation of the IFNγ cascade, thereby inducing apoptosis of infected cells, which may increase its immunogenicity via antigen cross-priming (16). Therefore, this vector can effectively deliver antigen to APC, such as dendritic cells (17). VEE virus-like replicon particles (VRP) can break immune tolerance in rats vaccinated against the *neu* molecule and can induce efficient immune responses to tumors (18). Given that VRP induce potent and protective immune responses in primates (19), they may be the ideal tool for vaccine delivery in humans.

In the current study, we used both prophylactic vaccination and therapeutic vaccination in prostate tumor-bearing mice to evaluate the effectiveness of STEAP delivery through DNA vectors and VRP. Our results show, for the first time in an *in vivo* system, that STEAP-based vaccination increases the overall survival rate of prostate tumor-bearing mice.

Materials and Methods

Plasmid DNA constructs and peptide synthesis. A DNA sequence encoding mouse STEAP was obtained from pCR-mSTEAP (11). For the generation of STEAP-expressing plasmid (pcDNA3-mSTEAP), *mSTEAP* DNA was amplified using two specific primers that included a *Hin*dIII and a *Xho*I site: 5′-CCCAAGCTTATGGAGATCAGTGACGAT-3′ and 5′-GGCGACTCCTC-AACCTGGAGGCCATCT-3′. Amplification was done for 30 s at 94°C, 30 s at 56°C, and 30 s at 72°C. An additional extension step was done for 10 min at 72°C. The PCR product was then cloned into the pcDNA3 expression vector (Invitrogen, Carlsbad, CA). The accuracy and correct open reading frame of the pcDNA3-mSTEAP construct were confirmed by DNA sequencing. pcDNA3-STEAP or an empty vector (pcDNA3) was transformed into TOP10 competent *Escherichia coli* (Stratagene, La Jolla, CA). Then, plasmid DNA copies were amplified in liquid culture and purified using an EndoFree plasmid maxi kit (Qiagen Sciences, MD). DNA used for vaccination had an A_{260}:A_{280} ratio of 1.9.

Replicon construction and VRP production. The *mSTEAP* gene was amplified by using specific primers: 5′-TGGAGATCAGTGACGAT-3′ and 5′-TTAATTAAGGCGAGCTCCTACAACC-3. A Pac-1 site was added to the antisense primer. Amplification was done for 30 s at 94°C, 30 s at 58°C, and 30 s at 72°C. An additional extension step was done for 10 min at 72°C. The PCR product was digested with the appropriate 3′ enzyme and ligated into the AlphaVax replicon vector plasmid (Research Triangle Park, NC), phosphorylated extracellular signal-regulated kinase, which is a derivative of pVR21 (20), digested with *Eco*RV and the matching 3′ enzyme. The presence of *mSTEAP* in the replicon plasmid was assessed by DNA sequencing.

Mice and cell lines. Pathogen-free, C57BL/6 and MLR/lpr mice were obtained from Taconic Farms (Germantown, NY). CD8 and CD4 knockout (KO) mice were purchased from The Jackson Laboratory (Bar Harbor, ME) and RAG KO mice were kindly donated by Chaim Jacob [University of Southern California (USC), Los Angeles, CA]. Mice were housed in the animal facilities of USC and they had food and water *ad libitum*. Research was conducted in compliance with institutional animal use guidelines. TRAMPC-2 prostate tumor cells were cultured in Iscove's modified Dulbecco's medium (IMDM) supplemented with 5% heat-inactivated FCS (JRH Biosciences, Lenexa, KS), 5% NuSerum (Collaborative Biomedical Products, Bedford, MA), 2 mmol/L L-glutamine, 100 μg/mL kanamycin, 0.01 nmol/L dihydrotestosterone (Sigma Chemical Co. St. Louis, MO), and 5 μg/mL insulin (Sigma Chemical). EL-4 cells obtained from the American Type Culture Collection (ATCC, Manassas, VA) were maintained in RPMI 1640 supplemented with 10% heat-inactivated FCS, 2 mmol/L L-glutamine, 100 μg/mL kanamycin, 50 mmol/L 2-mercaptoethanol, 1 mmol/L MEM sodium pyruvate, 0.1 mmol/L MEM nonessential amino acids, and 0.024 mmol/L sodium bicarbonate (Life Technologies, Gaithersburg, MD). RMA-S cells deficient in transporter associated with antigen processing and obtained from the ATCC were maintained in IMDM medium supplemented with 10% heat-inactivated FCS, 2 mmol/L L-glutamine, 100 μg/mL kanamycin, and 50 mmol/L 2-mercaptoethanol.

Peptides. Peptides were synthesized using standard methods at the Norris Cancer Center core facility at the University of Southern California. Peptides were dissolved at 29 mg/mL in DMSO (Sigma Chemical), aliquoted in a small volume, and stored at −70°C until further use.

Peptide binding assay. A MHC class I stabilization assay was done. RMA-S cells were incubated at 30°C overnight. Peptide at various concentrations was added for 1 h at 30°C and cells were incubated overnight at 37°C. Cells were stained on ice with FITC-antimouse H-2D^b or H-2K^b (BD PharMingen, San Diego, CA) for 30 min at 4°C. As a control, RMA-S cells were incubated with $E7_{49–57}$ (21) or $PSA_{(-3)-6}$ (VTWIGAAPL; ref. 22). Peptide binding was determined by flow cytometry using a Beckman Coulter Cytomic FC 500 cytometer equipped with CXP software (Beckman Coulter, Inc., Miami, FL). The fluorescence index was calculated according to the following formula: fluorescence index = (fluorescence after peptide stimulation / fluorescence without peptide stimulation) − 1.

VRP preparation. The procedures used for making VRP were based on a two helper system as described previously (20). Purified VRP were resuspended in an isotonic phosphate-buffered solution with 1% mouse serum (formulation buffer) and stored at −80°C until use.

DNA-gold preparation. DNA-coated gold particles were prepared by resuspending 25 mg of 1.0-μm gold microcarrier (Bio-Rad, Hercules, CA) in 100 μL of 0.05 mol/L spermidine (Sigma Chemical) and sonicating. Plasmid DNA (50 μg) was added to the microcarrier and this mixture was precipitated by addition of 1.0 mol/L $CaCl_2$ (100 μL) for 10 min. The precipitate was washed thrice with brand new absolute ethanol and it was resuspended in 3 mL polyvinylpyrrolidone (0.1 mg/mL; Bio-Rad) dissolved in absolute ethanol. The DNA-coated gold was loaded into the tubing and allowed to settle for 3 min. The ethanol was gently drawn out and the tubing was dried by nitrogen gas flowing at a rate of 0.3 L/min. Tubing was cut into 0.5-inch pieces placed in cartridges and stored at 4°C until use.

Enzyme-linked immunospot assay. Enzyme-linked immunospot assays were done as described previously (23), except that splenocytes were stimulated with $mSTEAP_{326–335}$ or human papillomavirus-16 (HPV-16) $E7_{49–57}$ peptide in the presence of 20 IU (infectious units)/mL interleukin (IL)-2 and spots were developed with 3-amino-9-ethyl-carbazole substrate (Sigma Chemical).

Cytotoxicity assay. A standard ^{51}Cr release assay was carried out as described previously (24), except that EL-4 cells were cultured overnight with either no peptide, $mSTEAP_{326–335}$, or an irrelevant peptide (HPV-16 $E7_{49–57}$), each at 10 μg/mL.

Immunization and tumor challenge. Male C57BL/6 mice were anesthetized i.p. with 2.4 mg ketamine (Phoenix Pharmaceuticals, Inc., St. Joseph, MO) and 480 μg xylazine (Phoenix Pharmaceuticals). DNA-coated gold particles were delivered to a shaved area on the abdomen using a helium-driven gene gun (Bio-Rad) with a discharge pressure of 400 p.s.i. Each mouse received 2 μg mSTEAP DNA vaccine. Fifteen days after gene gun vaccination, mice were s.c. boosted ~1 cm from the tail base with 10^6 IU mSTEAP-VRP or 2 μg mSTEAP DNA vaccine. Another group of mice was vaccinated and boosted with 10^6 IU mSTEAP-VRP. As a control group, mice were vaccinated with pcDNA3 or 10^6 IU green fluorescent protein (GFP)-VRP. Ten days after boosting, mice were challenged s.c. with 5×10^5 TRAMPC-2 cells resuspended in 100 μL HBSS (Sigma Chemical). For therapeutic vaccination, groups of mice were s.c. injected with 5×10^5

TRAMPC-2 cells resuspended in HBSS. At day 31, mice that had developed a palpable tumor received 2 μg mSTEAP DNA vaccine. Fifteen days later, they were boosted s.c. with 10^6 IU mSTEAP-VRP. VRP were injected as described above. Control groups of mice were immunized and boosted with pcDNA3 and GFP-VRP, respectively, or received no treatment. In all cases, tumor growth was monitored twice weekly with engineer calipers after challenge with TRAMPC-2 cells. Survival was followed until tumors reached volumes >1,000 mm^3.

Isolation of tumor-infiltrating lymphocytes and flow cytometry analysis. Tumor-infiltrating lymphocytes (TIL) were isolated from individual prostate tumors as described previously (25). TIL were analyzed by flow cytometry for CD3 and either CD4 or CD8 expression. 10^6 TIL were incubated in staining medium containing FcBlock receptor 2.4G2 for 10 min on ice followed by the addition of fluorochrome-conjugated antibodies (FITC-anti-CD3, PCy7-CD25, and PCy5-CD8/CD4; BD PharMingen) for 20 min at 4°C. Analysis was done on a Beckman Coulter FC 500 cytometer equipped with CXP software. The number of total cells per gram of tumor was calculated by multiplying the percentage of $CD3^+CD4^+$ or $CD3^+CD8^+$ cells by the total number of lymphocytes and dividing that number by 100. These numbers were divided by the mass of tumor to calculate the number of those TIL per gram of tumor.

Measurement of intratumoral cytokine expression. Tumors were collected, weighed, and homogenized in PBS containing 2× Halt Protease Inhibitor Cocktail (Pierce, Rockford, IL). One percent of bovine serum albumin (BSA; Sigma Chemical) was added and the supernatants were collected by centrifugation at 4°C for 20 min. The cytokine levels in the supernatants were quantified using the Bio-Plex mouse cytokine assay (Bio-Rad) and a Bio-Plex HTF system equipped with Bio-Plex Manager 4.0 software following the manufacturer's instructions.

Detection of rheumatoid factor and autoantibodies against ssDNA. Detection of autoantibodies to ssDNA was done as described previously (26). Nunc-Immuno Maxisorb plates (Nalgene International Research, Rochester, NY) were used. Salmon sperm DNA and BSA were obtained from Sigma. Horseradish peroxidase (HRP)–conjugated goat anti-mouse IgG was obtained from Southern Biotechnology Associates, Inc. (Birmingham AL). The absorbance of the colorimetric reaction was measured at a wavelength of 450 nm using an automated microplate reader (Bio-Rad). For the detection of rheumatoid factor, 2 μg/mL mouse IgG1κ (Sigma Chemical) was used for coating plates and HRP-conjugated goat anti-mouse IgM diluted at 1:2,000 was used as the detecting antibody (Southern Biotechnology Associates).

Histology and immunofluorescent staining. Kidney, prostate, and testis from immunized mice were fixed in 10% buffered formalin and embedded in paraffin. Five-micrometer sections were stained with H&E. For immunofluorescence, 5-μm cryosections were blocked with 0.5% rat serum (Vector Laboratories, Burlingame, CA) in PBS for 20 min. Endogenous biotin activity was blocked with a commercial Biotin-Avidin kit (Vector Laboratories). Sections were incubated during 1 h with biotin-conjugated rat anti-mouse primary antibodies that were visualized with streptavidin-conjugated to Alexa 488 or Alexa 594 (Molecular Probes, Carlsbad, CA). Tissue-specific autoantibodies directed against self-antigens expressed in kidney, prostate, testis, and thymus from RAG mice were detected by immunofluorescence as described previously (27). Accumulation of IgM and collagen deposition in kidneys was analyzed by immunohistochemistry as described previously (28), except that endogenous peroxidase was blocked with 6% H_2O_2 in methanol for 30 min. Each tissue was incubated for 1 h at room temperature with biotinylated antimouse IgM (BD PharMingen) or polyclonal rabbit anti-mouse collagen type IV (Abcam, Cambridge, MA). Rabbit polyclonal antibodies were detected with a biotinylated goat anti-rabbit antibody, streptavidin-coupled HRP, and 3,3′-diaminobenzidine (Sigma) as the chromogen. Tissue sections were counterstained with Gill's hematoxylin (Surgipath, Richmond, IL) and mounted with Vectamount resin (Vector Laboratories).

STEAP expression in the tissues of C57BL/6 mice was detected by immunofluorescence. Five-micrometer frozen sections were blocked with protein block serum-free (DAKO Corp., Carpinteria, CA) for 10 min at room temperature. Endogenous biotin activity was blocked as described above. Tissue sections were incubated for 1 h with a rabbit polyclonal antimouse

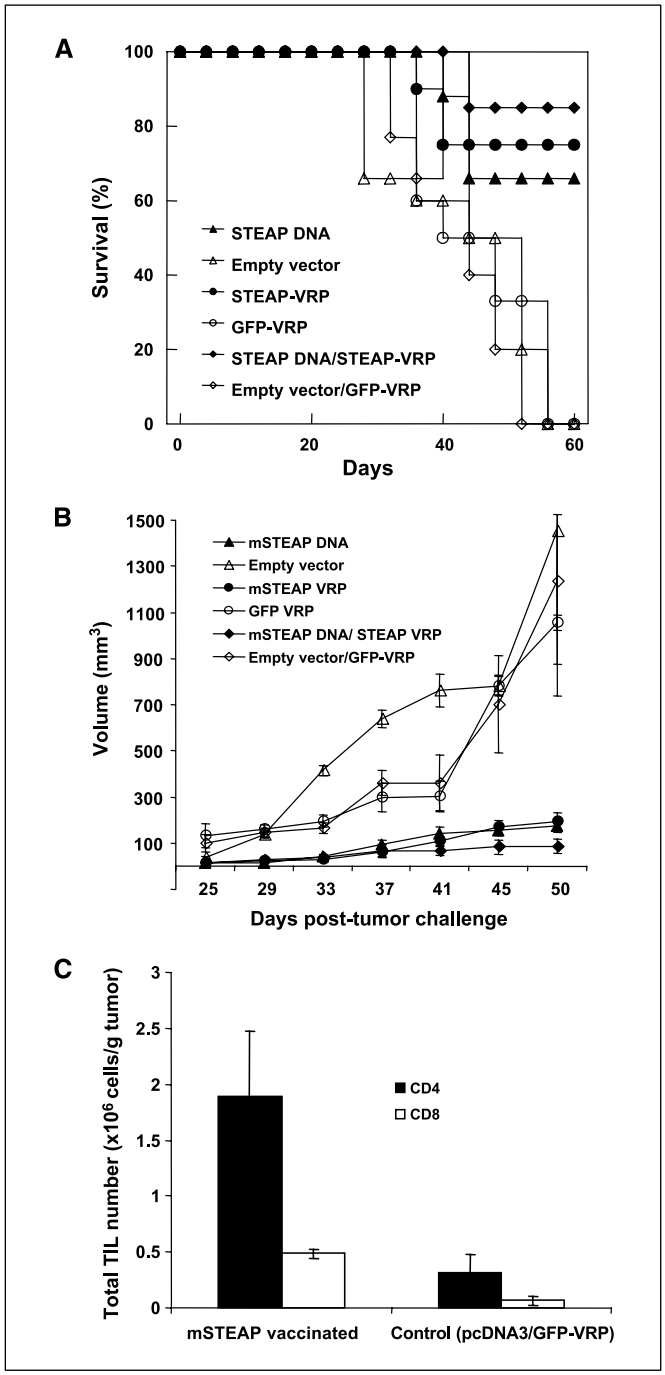

Figure 1. mSTEAP vaccination induced protection against tumor challenge. *A,* male C57BL/6 mice were vaccinated and boosted with pcDNA-mSTEAP (▲), s.c. with 10^6 IU mSTEAP-VRP (●), or with a combined vaccination protocol with pcDNA-mSTEAP followed by mSTEAP-VRP (♦). In control groups, mice were vaccinated and boosted with empty vector (Δ) and GFP-VRP (○) or vaccinated with empty vector and boosted with GFP-VRP (◇). Ten days after second vaccination, mice were challenged with 5×10^5 TRAMPC-2 cells and tumor protection was evaluated by following survival of nine vaccinated mice per experimental condition. *B,* tumor growth in mSTEAP-vaccinated mice. C57BL/6 mice were vaccinated as was described above. At day 25 postchallenge, tumor growth was monitored twice at week with engineer calipers. Data of one of two separate experiments with similar results. *Points,* mean of nine mice. *Bars,* SE. *C,* mSTEAP-vaccinated mice using a prime-boost scheme have increased numbers of $CD4^+$ and $CD8^+$ T cells in their tumor environment. TIL were recovered from fresh tumor, stained with antimouse CD4 PE or CD8a PE, and analyzed by flow cytometry. Absolute numbers of positive cells per tumor were calculated and normalized per gram of tumor. Representative of two independent experiments with similar results. *Columns,* mean of four mice; *bars,* SE.

Table 1. Stabilization of cell surface MHC by STEAP peptides

Peptide	Sequence	Score, predicted $T_{(1/2)}$, (min)	H2 molecule selected	Fluorescence index
$mSTEAP_{83–91}$	SLTFLYTLL	22	K_b	0.1
$mSTEAP_{186–193}$	RSYRYKLL	132	K_b	5
$mSTEAP_{326–335}$	DVSKINRTEM	240	D_b	16
$mSTEAP_{5–13}$	DDVTNPEQL	600	D_b	1
$E7_{49–57}$	RAHYNIVTF	3	D_b	7
$PSA_{(-3)–6}$	VTWIGAAPL	4	K_b	5

NOTE: MHC binding assays were done by loading RMA-S cells with the peptides indicated and by assessing the level of MHC-I by flow cytometry. The fluorescence index was calculated as described in Materials and Methods. Scores were obtained using an online HLA peptide binding prediction program (http://bimas.cit.nih.gov/).

STEAP, previously produced in our laboratory in rabbits immunized with a synthetic peptide (WKMKPKGNLEDDSYS). Bound antibodies were detected with biotinylated antirabbit (Vector Laboratories) and streptavidin conjugated to Alexa 488. Tissue sections were mounted with mounting medium for fluorescence with 4′,6-diamidino-2-phenylindole (Vector Laboratories).

Statistical analysis. Tumor growth, CTL responses, and absolute number of T cells were analyzed by a two-tailed paired Student's t test. ELISPOT data were analyzed by one-tailed Student's t test.

Results

mSTEAP expression in C57BL/6 mouse tissues. It has been shown previously by reverse transcription-PCR (RT-PCR) that mSTEAP is expressed in some normal mouse tissues (11). We have developed a STEAP-specific antibody, allowing us to analyze mSTEAP production in several tissues by immunofluorescence (Supplementary Data). mSTEAP was detected in prostate epithelial cells using this method, confirming our previous RT-PCR data. mSTEAP protein was absent in other tissues, including brain, muscle, heart, liver, salivary gland, and stomach. No positive staining was detected when an isotype control antibody was used, confirming the specificity of the anti-mSTEAP antibody. mSTEAP was expressed by splenic macrophages, as shown by the isolation of adherent cells, CD11b detection, and cloning and sequencing of this self-antigen (data not shown). In addition, mSTEAP was found in the thymic medulla, where STEAP-specific thymocytes may undergo the process of negative selection.

Prophylactic vaccination with mSTEAP delays tumor growth and improves survival. The efficacy of antigen-specific vaccination was evaluated by monitoring survival of immunized mice after challenge with tumor cells. Survival was significantly prolonged in mice vaccinated with mSTEAP using DNA, VRP, or a combined strategy after tumor challenge compared with control mice (Fig. 1*A*). Although all STEAP-based vaccination strategies significantly slowed tumor growth in tumor-challenged mice, DNA vaccination followed by boosting with VRP was the most effective way of inducing protective immunity (Fig. 1*B*). Based on these data, we selected the prime/boost (DNA/VRP) schedule for subsequent experiments. The protection induced by the vaccination correlated with an increase in the number of tumor-infiltrating CD4 and CD8 T cells as detected by flow cytometry (Fig. 1*C*).

STEAP vaccination induces antigen-specific CD8 T cells. The killing of transformed cells by antigen-specific CD8 T cells plays a central role in control of tumor growth. We evaluated whether STEAP-specific CD8 T cells capable of producing IFNγ were generated in response to vaccination. This cytokine is crucial for type 1 immune responses and is required for the activation of cytolytic functions in the CD8 population. Given that TRAMPC-2 cells express low levels of MHC class I, they were not able to activate purified T cells after IFNγ treatment *in vitro* (data not shown). To circumvent this, we identified mSTEAP peptides that could potentially bind to MHC class I molecules H-2D^b or H-2K^b. We selected four peptides based on the highest score of peptide/MHC class I half-life of dissociation predicted using the Parker automated program (29) and evaluated their capacity to stabilize MHC class I on RMA-S cells. $mSTEAP_{326–335}$ had a stronger affinity than $mSTEAP_{186–194}$, $STEAP_{83–91}$, and $STEAP_{5–13}$, (Table 1). $mSTEAP_{326–335}$, $mSTEAP_{186–194}$, and $STEAP_{5–13}$ were selected for analyzing the specific CD8 T-cell response by ELISPOT assay (Fig. 2*A*). $STEAP_{83–91}$ was not included in subsequent assays due to its low fluorescence index. Splenocytes from mSTEAP-vaccinated mice stimulated with mSTEAP peptides contained significant numbers of IFNγ-producing $mSTEAP_{326–335}$-specific CD8 T cells. Peptide-specific IFNγ-producing CD8 T cells were completely absent in mice vaccinated with an empty plasmid and GFP-VRP ($P < 0.05$, two tailed). The increased numbers of IFNγ$^+$ CD8 T cells found in vaccinated mice correlated with increased CTL activity as detected by chromium release assay using $mSTEAP_{326–335}$ (Fig. 2*B*).

Participation of CD4 and CD8 T cells. To determine the role of antigen-specific CD8 and CD4 T cells induced by vaccination, we followed tumor growth after challenging vaccinated C57BL/6 and CD4- or CD8-deficient mice with tumor cells. Mice were vaccinated with mSTEAP-(11)DNA, boosted with mSTEAP-VRP and challenged with TRAMPC-2 cells. Compared with tumor growth in C57BL/6 mice, tumor growth in vaccinated CD8KO mice was significantly delayed ($P = 0.001$, two tailed), whereas tumor growth was significantly accelerated in vaccinated CD4KO mice ($P = 0.004$, two tailed; Fig. 3*A*). These findings indicate that CD4 T cells participate in the control of tumor growth. There was no local production of protective cytokines [IL-2, IL-12p70, IFNγ, and tumor necrosis factor-α (TNF-α)] in mice lacking CD4 T cells (Fig. 3*B*). These protective cytokines were readily detectable in C57BL/6 and CD8KO mice and were produced at similar levels, with the exception that IL-2 was elevated in CD8KO mice (Fig. 3*B*).

Therapeutic vaccination with mSTEAP modestly controls the growth of well-established tumors. To assess the therapeutic efficacy of mSTEAP vaccination, tumor-bearing mice were immunized at day 31 with mSTEAP cDNA followed by a s.c. injection of mSTEAP-VRP at day 46. STEAP vaccination induced a

short but statistically significant delay in tumor growth ($P = 0.022$, two tailed) compared with a group of unvaccinated mice and a group of mice vaccinated with empty vector and GFP-VRP (Fig. 4).

Autoimmune reactions after vaccination with self-antigens. Given that mSTEAP is a self-antigen, mSTEAP-based vaccination has the potential risk of breaking immune tolerance and thus inducing an autoimmune process. Therefore, we analyzed production of two kinds of autoantibodies (rheumatoid factor and anti-ssDNA antibodies) in the serum of vaccinated mice and the presence of inflammatory cells in mSTEAP-expressing tissues. As a positive control for autoimmunity, we used serum and tissues from aged MRL/lpr mice. Although mSTEAP vaccination induced a low but detectable quantity of anti-ssDNA autoantibodies and low levels of rheumatoid factor, at day 84 after vaccination, the levels were minor compared with control aged MRL/lpr mice (Fig. 5*A*). Under physiologic conditions, autoantibodies are detectable without development of pathologic autoimmunity. The accumulation of IgM (possibly rheumatoid factor), the presence of inflammatory infiltrates, and collagen deposition were also analyzed in several tissues where STEAP is normally expressed at low levels, including kidney, testis, and prostate. Control MRL/lpr mice had accumulation of IgM and cell infiltrates in the kidney and had considerable kidney damage indicated by zones showing massive collagen deposition (Fig. 5*B*). In contrast, vaccinated mice did not have any signs of an active autoimmune pathology. No damage, infiltration, or autoimmunity was detected in testis or prostate after vaccination (data not shown). To determine whether the mSTEAP DNA/VRP vaccination regimen induced production of autoantibodies against self-antigens via bystander activation, we tested for the presence of autoantibodies that recognize self-antigens in the serum of vaccinated mice. Briefly, kidneys, prostate, or testes from RAG KO mice, which do not produce endogenous antibodies, were incubated with serum from vaccinated mice, and autoantibodies to self-antigens were detected with a FITC-conjugated antimouse IgG. No serum autoantibodies against self-antigens expressed in kidney, prostate, and testis were detected in control or vaccinated mice. In contrast, serum obtained from MRL/lpr mice contained a significant level of autoantibodies, which bound to different cells and structures in tissues of RAG mice (Fig. 5*C*).

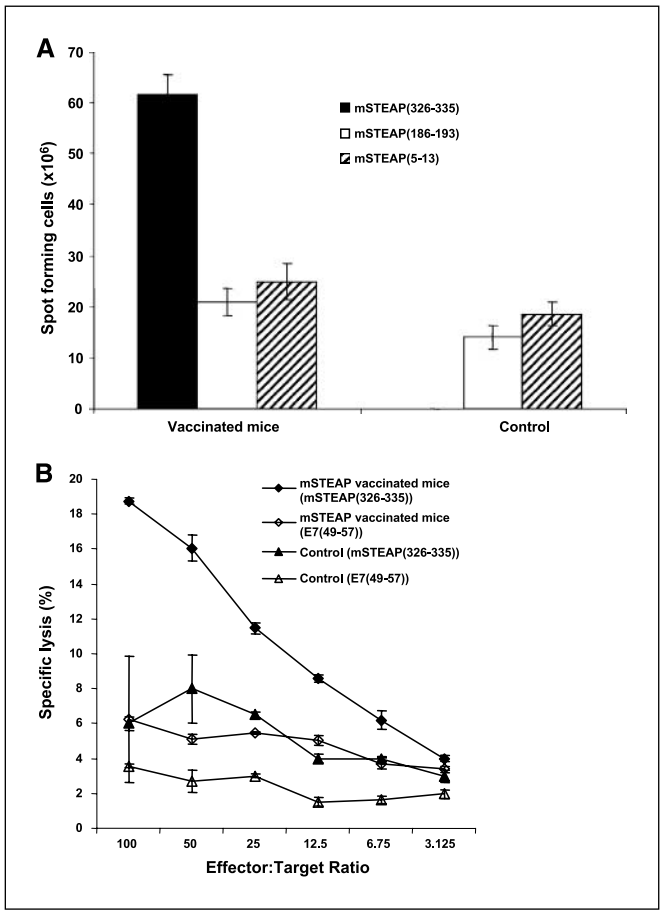

Figure 2. Characterization of the cellular response induced in the spleens of vaccinated mice after using gene gun or VRP as delivery systems. *A,* ELISPOT. T cells from mice vaccinated with mSTEAP-pcDNA3/mSTEAP-VRP or pcDNA3/GFP-VRP were activated with 10^6 spleen cells loaded with $mSTEAP_{326–335}$ peptide, $mSTEAP_{186–93,}$ $mSTEAP_{5-13}$, or in the presence of 5 IU IL-2 over 48 h. The results are presented as spot-forming cells per 10^6 splenocytes. *Columns,* mean of four mice; *bars,* SE. *B,* chromium-release assay. T cells from mSTEAP-vaccinated mice (♦) or control group (▲) were stimulated for 5 d with 10^6 spleen cell loaded with $mSTEAP_{326–335}$ peptide in the presence of 20 IU IL-2. Cells were then cultured with ^{51}Cr-labeled EL-4 targets pulsed with $mSTEAP_{326–335}$ (♦ and ▲) or control HPV-16 $E7_{49–57}$ (◇ and Δ) peptide at the indicated E:T ratios. Specific lysis was calculated as described previously. *Points,* mean of three pools of three mice each; *bars,* SE.

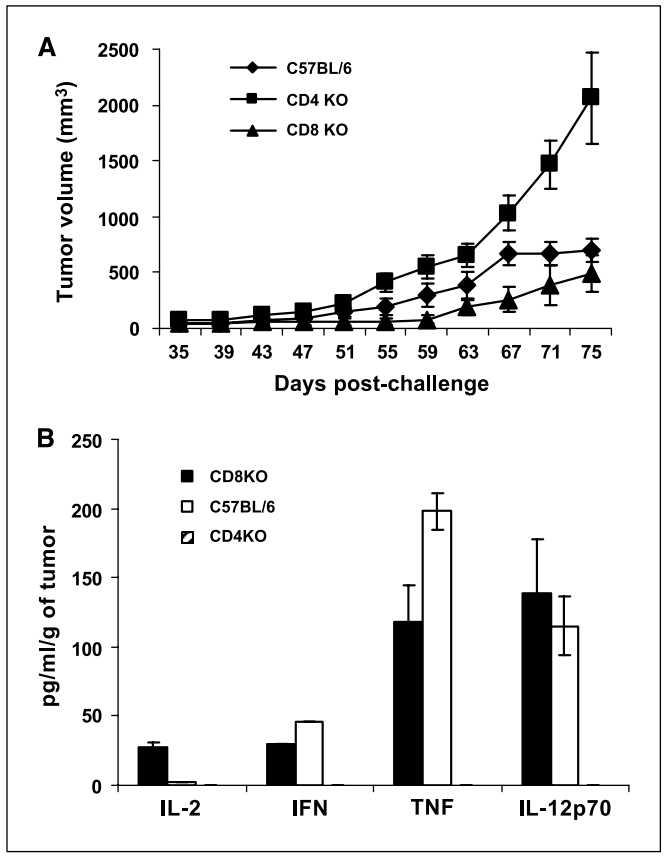

Figure 3. The roles of CD4 and CD8 T cells in the control of growth of s.c. implanted prostate tumor cells. *A,* CD4 T cells play a main role in the control of tumor growth. Groups of 10 wild-type C57BL/6, CD8KO, and CD4KO mice were vaccinated with mSTEAP-pcDNA, boosted with mSTEAP-VRP, and challenged with TRAMPC-2 cells. Tumor growth was monitored twice weekly. *Points,* mean of 10 mice; *bars,* SE. *B,* mSTEAP vaccination induces Th1 cytokines. Tumors were collected, weighed, and homogenized with a polytron. The amounts of cytokines in supernatants obtained from the tumors of vaccinated C57BL/6, CD8KO, and CD4KO mice were quantified using a Bio-Plex HTF system equipped with Bio-Plex Manager 4.0 software. Data are shown as total number cells per gram of tumor. *Columns,* mean of eight mice; *bars,* SE.

Discussion

In the current study, we have assessed efficacy of several prime-boost immunotherapy strategies directed against STEAP in a mouse model of prostate cancer. STEAP is a member of the metalloreductase family (30) that lacks the NH_2-terminal oxidoreductase domain and currently has no defined enzymatic function. Human STEAP is expressed in the prostate (10) and has been implicated in prostate cancer metastasis. Previously, we detected STEAP mRNA in different tissues from normal mice (11). Here, we show that mSTEAP is a membrane protein produced in kidney, spleen, thymus, testis, and prostate. Detection of mSTEAP mRNA in macrophages indicates that it is endogenously expressed by these APC rather than being picked up by them elsewhere for presentation to T cells. Therefore, mSTEAP may have an important role during macrophage activation or maturation. Thymic STEAP expression suggests selection of the mature TCR repertoire via interaction between STEAP peptide and MHC complex molecules during thymic differentiation. However, self-reactive CD8 T cells able to recognize STEAP-expressing tumor cells were detected in the peripheral T-cell pool, indicating that negative selection is not completely effective (12). In general, these autoreactive CD8 T cells are controlled in the periphery by several regulatory mechanisms, including deletion, anergy, phenotypic skewing, and regulatory T-cell activity (31).

The antigen delivery systems most commonly used to induce protective immunity against infectious agents and transformed cells are based on administration of plasmids by gene gun or inoculation of viral vectors containing the gene of interest. However, prime-boost schemes, where DNA and viruses are inoculated in succession, often induce the best immunity (15, 32). We used VEE VRP in our vaccination schemes in combination with DNA vaccination. Consistent with previous reports, we found the best tumor immunity and protection in the group of mice vaccinated with DNA and VRP.

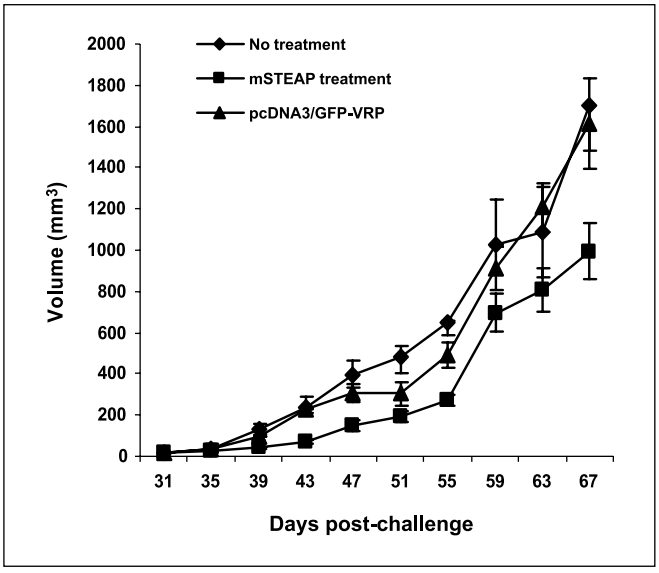

Figure 4. Therapeutic vaccination with mSTEAP did not completely control tumor growth in preexisting tumors. Three different groups of male C57BL/6 mice were inoculated with TRAMPC-2 cells. At day 31, all the mice had a palpable tumor. In one group, mice were vaccinated pcDNA-mSTEAP and mSTEAP-VRP. In control group, mice received a shot of empty vector followed by a boost with GFP-VRP. A third group did not receive any treatment. Tumor growth was monitored twice weekly. Data of one of two separate experiments with similar results. *Points,* mean of 10 mice; *bars,* SE.

Due to the relevance of IFNγ in cellular immunity, we evaluated the production of this cytokine by STEAP-specific splenic CD8 T cells after vaccination. CD8 T cells from vaccinated mice were able to produce IFNγ after activation with the specific peptide $mSTEAP_{326–335}$. It is unknown whether there are other populations of CD8 T cells that can recognize other peptides (12), contribute to the lysis of transformed cells, and aid the generation of an adequate type 1 T-cell environment, events that are crucial for the control of tumor growth. Furthermore, CD4 T cells activated by class II-restricted peptides presented on the surface of APC (33) may produce IFNγ and contribute to tumor killing. Nevertheless, IFNγ production was correlated with the *in vitro* cytolytic activity of CD8 T cells toward target cells loaded with the specific peptide $mSTEAP_{326–335}$, indicating that STEAP-specific CTL are being induced in our model.

Protection was associated with considerable T-cell infiltration of the tumors of vaccinated mice. The majority of TIL were CD4 T cells, as determined by flow cytometry and immunofluorescence. The attraction of Th1 and Tc1 to a common place in the tumor is critical to induce the activation of CD8 CTL that mediate tumor cell killing (34). To determine the contribution of CD4 and CD8 T cells to the clearance of prostate transplantable tumors in vaccinated mice, we monitored tumor growth in vaccinated CD4KO and CD8KO mice deficient in CD4 or CD8 T cells. We hypothesized that the CD8 T-cell population was most important to tumor rejection. Furthermore, we predicted that the response would be more efficient in CD4KO mice due to the absence of natural regulatory T cells (35). Surprisingly, CD8KO mice were more efficient than CD4KO mice in controlling tumor growth. Taken together, our data suggest that CD4 Th1 cells play an active role in the control of transformed cells and that minimal negative modulation of the immune response by regulatory CD4 T cells occurs in our model (36). It has been shown by several groups that proinflammatory cytokines have a central role in the generation of protective tumor immunity. For example, IL-12 secreted by activated dendritic cells is important for local Th1 and Tc1 differentiation. In addition, IL-12 acts in combination with IL-2 to play a role in initiating the development of effector functions of CD8 T cells and generation of memory CD8 T cells (37). IL-12 is also important for promoting IFNγ production by TIL. IFNγ is fundamental to the control of tumor growth by promoting the generation of strong cellular immune responses against transformed cells and by inhibiting tumor angiogenesis (38). A combination of TNF-α derived from CD4 T cells and IFNγ is required for the activation of macrophages and neutrophils. These cells produce molecules that are toxic to malignant cells, such as nitric oxide, superoxide, and hydrogen peroxide. IFNγ is also responsible for the induction of chemokines, such as CXCL9, CXCL10, and CXCL11, which attract Th1 and Tc1 cells to the tumor (39). The dominance of proinflammatory cytokines, such as IL-12, IL-2, TNF-α, and IFNγ, in the tumors of C57BL/6 and CD8KO mice suggests that control of tumor growth is taking place. In our model, the increased production of IL-12 in CD8KO and C57BL/6 mice is associated with the presence of tumor-infiltrating mature dendritic cells. Maturation of dendritic cells may be a direct consequence of the considerable production of TNF-α in the tumor microenvironment. Tumor-produced IL-12 is likely responsible for the increased local production of IFNγ. Due to the detection of these cytokines in CD8KO mice and their complete absence in CD4KO mice, we propose that IFNγ, IL-2, and TNF-α are derived mainly from CD4 T cells. Given that CD4 T helper cells are required for licensing dendritic cells (40), the lack of intratumoral IL-12 in CD4KO mice indicates that IL-12 is likely to be produced by mature dendritic cells at the site of tumor growth.

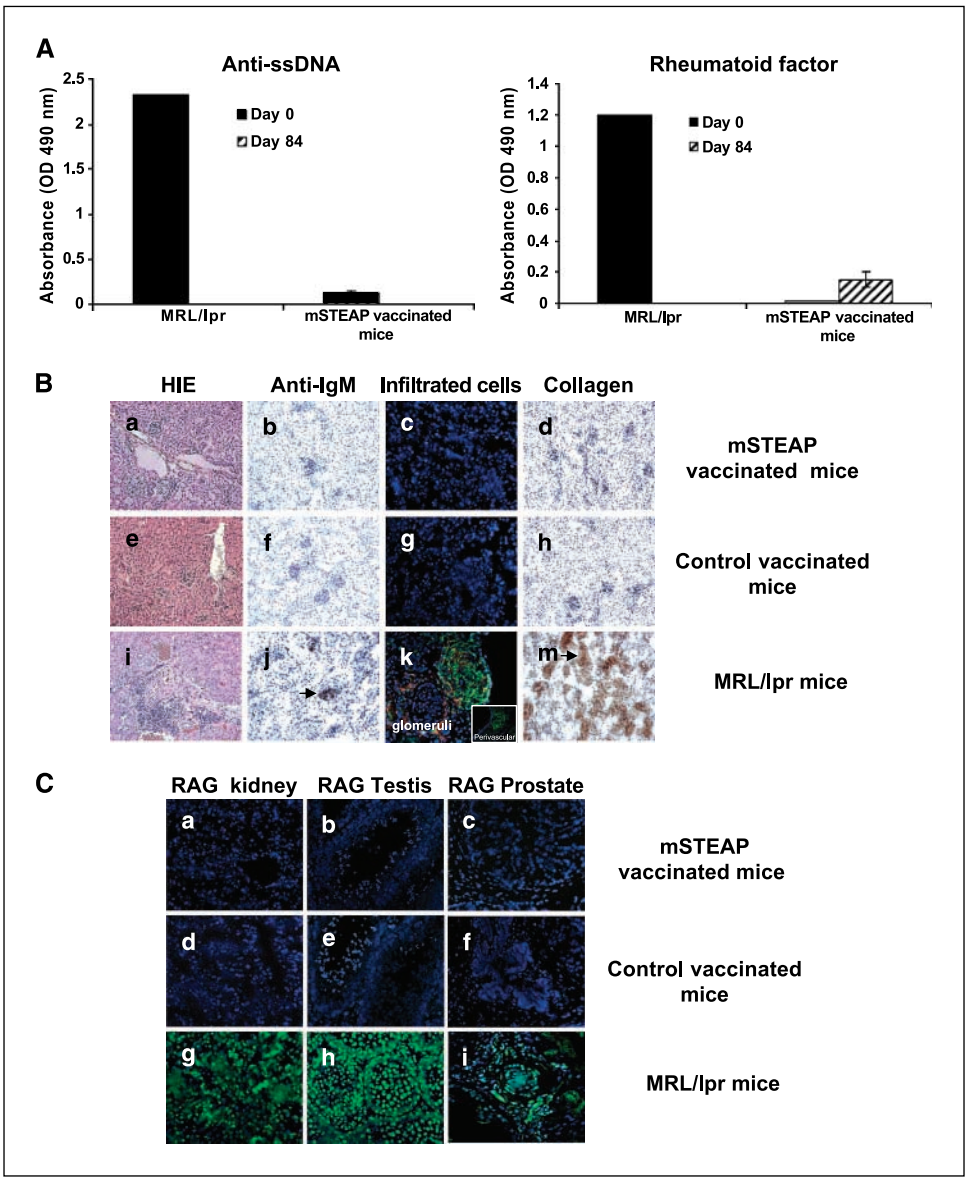

Figure 5. mSTEAP vaccination did not induce any signs of autoimmunity. *A,* autoantibody production in serum samples from male C57BL/6 mice immunized with mSTEAP. Anti-ssDNA antibodies and rheumatoid factor were measured in serum from mSTEAP-vaccinated and control group by ELISA and titers were compared with a serum sample from MLR/lpr mice (positive control of active autoimmunity). Data of one of two similar independent experiments. *Columns,* mean of eight mice; *bars,* SE. *B,* absence of inflammation and cell infiltrates in kidney from mSTEAP-vaccinated C57BL/6 mice. A complete absence of inflammatory cells (*a* and *c*) was observed in a kidney section taken at day 50 after vaccination (mSTEAP-DNA and mSTEAP-VRP) and stained with H&E. Control mice did not show any significant cell infiltration (*e* and *g*) compared with the massive inflammatory infiltration seen in MLR/lpr mice (*i* and *k*). Inflammatory infiltrates were primarily composed of macrophages, T cells, and dendritic cells (*k*). Immunohistochemistry analysis showed IgM deposition on glomerular basement membrane in MLR/lpr (*j*), which also had a considerable collagen deposition (*m*). No positive stain was detected in kidney from mSTEAP-vaccinated (*b* and *d*) or control mice (*g* and *h*). Representative images of similar lesions found in an experimental group of eight mice. Images were captured at ×20 magnification. *C,* mSTEAP vaccination does not induce autoantibodies against self-antigens in tissues where STEAP is expressed. Frozen sections of kidney, testis, and prostate from RAG mice were incubated with serum from mSTEAP-vaccinated or control group and bound antibodies were detected with a FITC-antimouse IgG antibody. Neither mSTEAP-vaccinated mice (*a–c*) nor the control group (*d–f*) showed any positive reaction against self-antigen present on those tissues. In contrast, tissues from MLR/lpr mice show a strong positive reaction against self-components of STEAP-expressing organs (*g–i*).

Other strategies to induce tumor immunity have also failed to mediate complete tumor rejection and have only delayed tumor growth (41, 42). Recently, it was shown that orthotopically implanted TRAMPC-1P3 tumors developed an immunosuppressive microenvironment where dendritic cells failed to express costimulatory molecules and class II antigens, interfering with adequate T-cell activation (43). Given that TRAMPC-1 and TRAMPC-2 cell lines were derived from the prostate tumor of a male TRAMP mouse (44) and that the tumor growth kinetics follow the same pattern, it is possible that mSTEAP treatment at day 31 was too late to modify the tumor microenvironment, resulting in unsuccessful treatment. Recently, it was shown that peritumoral injection at day 17, 20, and 23 of an adenoviral vector-expressing murine CD40L in preestablished TRAMPC-2 tumors only delayed tumor growth in five of six mice and complete tumor inhibition was detected only in one mouse (45). In other tumor models where mice were treated at 3, 4, or 7 days after tumor injection, a higher therapeutic success rate was achieved (42, 46). These findings support the idea that early treatment of TRAMPC-2 tumors could improve the efficacy of mSTEAP treatment.

We chose to inoculate mice with 10^6 IU VRP-STEAP based on our previous findings (47) and those of others (18). However, in other prime-boost schemes, 10^7 plaque-forming units induced protection against VEE virus and HPV-16 tumors, respectively (48). Therefore, we speculate that higher or multiple doses of VRP-STEAP may induce better tumor immunity in future studies.

Due to the self-nature of STEAP, the presence of CpG in the DNA, and the use of a viral vector capable of activating autoreactive lymphocytes, vaccinated mice were monitored for indicators of active autoimmunity. Although low levels of autoantibodies were detected, they were significantly lower than those detected in MLR/lpr mice (49). IgM accumulation and collagen deposition in kidneys were detected only in MLR/lpr mice as described previously (50). Furthermore, lymphocyte infiltration was not detected in STEAP-expressing healthy tissues, suggesting STEAP vaccination under these experimental conditions is safe. However, development of autoimmunity may still occur if another vaccination scheme that is able to eradicate tumors is used.

We conclude that STEAP-DNA vaccination combined with STEAP-VRP boosting can induce a STEAP-specific immune response that is able to delay tumor growth without promoting pathologic autoimmunity. Combination of this basic vaccination scheme with additional immunomodulation may be capable of completely eradicating prostate tumors, allowing the translation of this immunotherapy into the clinical arena.

Acknowledgments

Received 8/31/2006; revised 10/31/2006; accepted 11/27/2006.

Grant support: Department of Defense grants DAMD 17-02-1-0244 and DAMD PC041078 and NIH training grant T32 GM 067587 (A. Gray). W. Martin Kast holds the Walter A. Richter Cancer Research Chair.

The costs of publication of this article were defrayed in part by the payment of page charges. This article must therefore be hereby marked *advertisement* in accordance with 18 U.S.C. Section 1734 solely to indicate this fact.

References

1. Jemal A, Thomas A, Murray T, Thun M. Cancer statistics, 2002. CA Cancer J Clin 2002;52:23–47.
2. Crawford ED, Rosenblum M, Ziada AM, Lange PH. Hormone refractory prostate cancer. Urology 1999;54:1–7.
3. Hillman GG, Triest JA, Cher ML, Kocheril SV, Talati BR. Prospects of immunotherapy for the treatment of prostate carcinoma-a review. Cancer Detect Prev 1999; 23:333–42.
4. Tannock IF, Osoba D, Stockler MR, et al. Chemotherapy with mitoxantrone plus prednisone or prednisone alone for symptomatic hormone-resistant prostate cancer: a Canadian randomized trial with palliative end points. J Clin Oncol 1996;14:1756–64.
5. Woods GM, Malley RC, Muller HK. The skin immune system and the challenge of tumour immunosurveillance. Eur J Dermatol 2005;15:63–9.
6. Noguchi M, Kobayashi K, Suetsugu N, et al. Induction of cellular and humoral immune responses to tumor cells and peptides in HLA-A24 positive hormone-refractory prostate cancer patients by peptide vaccination. Prostate 2003;57:80–92.
7. Ross S, Spencer SD, Holcomb I, et al. Prostate stem cell antigen as therapy target: tissue expression and *in vivo* efficacy of an immunoconjugate. Cancer Res 2002;62: 2546–53.
8. Zhu ZY, Zhong CP, Xu WF, et al. PSMA mimotope isolated from phage displayed peptide library can induce PSMA specific immune response. Cell Res 1999; 9:271–80.
9. Wang Y, Harada M, Yano H, et al. Prostatic acid phosphatase as a target molecule in specific immunotherapy for patients with nonprostate adenocarcinoma. J Immunother 2005;28:535–41.
10. Hubert RS, Vivanco I, Chen E, et al. STEAP: a prostate-specific cell-surface antigen highly expressed in human prostate tumors. Proc Natl Acad Sci U S A 1999; 96:14523–8.
11. Yang D, Holt GE, Velders MP, Kwon ED, Kast WM. Murine six-transmembrane epithelial antigen of the prostate, prostate stem cell antigen, and prostate-specific membrane antigen: prostate-specific cell-surface antigens highly expressed in prostate cancer of transgenic adenocarcinoma mouse prostate mice. Cancer Res 2001;61:5857–60.
12. Rodeberg DA, Nuss RA, Elsawa SF, Celis E. Recognition of six-transmembrane epithelial antigen of the prostate-expressing tumor cells by peptide antigen-induced cytotoxic T lymphocytes. Clin Cancer Res 2005;11:4545–52.
13. Alves PM, Faure O, Graff-Dubois S, et al. STEAP, a prostate tumor antigen, is a target of human CD8 (+) T cells. Cancer Immunol Immunother 2006;55:1515–23.
14. Mwau M, Cebere I, Sutton J, et al. A human immunodeficiency virus 1 (HIV-1) clade A vaccine in clinical trials: stimulation of HIV-specific T-cell responses by DNA and recombinant modified vaccinia virus Ankara (MVA) vaccines in humans. J Gen Virol 2004;85:911–9.
15. Cassetti MC, McElhiney SP, Shahabi V, et al. Antitumor efficacy of Venezuelan equine encephalitis virus replicon particles encoding mutated HPV16 E6 and E7 genes. Vaccine 2004;22:520–7.
16. Leitner WW, Hwang LN, deVeer MJ, et al. Alphavirus-based DNA vaccine breaks immunological tolerance by activating innate antiviral pathways. Nat Med 2003;9:33–9.
17. MacDonald GH, Johnston RE. Role of dendritic cell targeting in Venezuelan equine encephalitis virus pathogenesis. J Virol 2000;74:914–22.
18. Wang X, Wang JP, Maughan MF, Lachman LB. Alphavirus replicon particles containing the gene for HER2/*neu* inhibit breast cancer growth and tumorigenesis. Breast Cancer Res 2005;7:R145–55.
19. Davis NL, Caley IJ, Brown KW, et al. Vaccination of macaques against pathogenic simian immunodeficiency virus with Venezuelan equine encephalitis virus replicon particles. J Virol 2000;74:371–8.
20. Pushko P, Parker M, Ludwig GV, Davis NL, Johnston RE, Smith JF. Replicon-helper systems from attenuated Venezuelan equine encephalitis virus: expression of heterologous genes *in vitro* and immunization against heterologous pathogens *in vivo*. Virology 1997;239:389–401.
21. Feltkamp MC, Smits HL, Vierboom MP, et al. Vaccination with cytotoxic T lymphocyte epitope-containing peptide protects against a tumor induced by human papillomavirus type 16-transformed cells. Eur J Immunol 1993;23:2242–9.
22. Koh YT, Higgins SA, Weber JS, Kast WM. Immunological consequences of using three different clinical/laboratory techniques of emulsifying peptide based vaccines in incomplete Freund's adjuvant. J Transl Med 2006;4:42.
23. Wakabayashi MT, Da Silva DM, Potkul RK, Kast WM. Comparison of human papillomavirus type 16 L1 chimeric virus-like particles versus L1/L2 chimeric virus-like particles in tumor prevention. Intervirology 2002;45:300–7.
24. Eiben GL, Velders MP, Schreiber H, et al. Establishment of an HLA-A*0201 human papillomavirus type 16 tumor model to determine the efficacy of vaccination strategies in HLA-A*0201 transgenic mice. Cancer Res 2002;62:5792–9.
25. Garcia-Hernandez ML, Hernandez-Pando R, Gariglio P, Berumen J. Interleukin-10 promotes B16-melanoma growth by inhibition of macrophage functions and induction of tumour and vascular cell proliferation. Immunology 2002;105:231–43.
26. Coligan JE, Bierer BE, Margulies DH, Shevach EM, Strober W, editors. Current protocols in immunology. Indianapolis (IN): John Wiley & Sons; 2006. p. 15.20.02–06.
27. Kojima H, Gu H, Nomura S, et al. Abnormal B lymphocyte development and autoimmunity in hypoxia-inducible factor 1α -deficient chimeric mice. Proc Natl Acad Sci U S A 2002;99:2170–4.
28. D'Andrea MR. Collagenase predigestion on paraffin sections enhances collagen immunohistochemical detection without distorting tissue morphology. Biotech Histochem 2004;79:55–64.
29. Parker KC, Bednarek MA, Coligan JE. Scheme for ranking potential HLA-A2 binding peptides based on independent binding of individual peptide side-chains. J Immunol 1994;152:163–75.
30. Ohgami RS, Campagna DR, McDonald A, Fleming MD. The Steap proteins are metalloreductases. Blood 2006;108:1388–94.
31. Walker LS, Abbas AK. The enemy within: keeping self-reactive T cells at bay in the periphery. Nat Rev Immunol 2002;2:11–9.
32. Mackova J, Stasikova J, Kutinova L, et al. Prime/boost immunotherapy of HPV16-induced tumors with E7 protein delivered by Bordetella adenylate cyclase and modified vaccinia virus Ankara. Cancer Immunol Immunother 2006;55:39–46.
33. Harada M, Matsueda S, Yao A, Noguchi M, Itoh K. Vaccination of cytotoxic T lymphocyte-directed peptides elicited and spread humoral and Th1-type immune responses to prostate-specific antigen protein in a prostate cancer patient. J Immunother 2005;28:368–75.
34. Ciavarra RP. T helper cells in cytotoxic T lymphocyte development: analysis of the cellular basis for deficient T helper cell function in the L3T4-independent T helper cell pathway. Cell Immunol 1991;134:427–41.
35. Piccirillo CA, Shevach EM. Control of $CD8^+$ T cell activation by $CD4^+CD25^+$ immunoregulatory cells. J Immunol 2001;167:1137–40.
36. Noble A, Giorgini A, Leggat JA. Cytokine-induced IL-10-secreting CD8 T cells represent a phenotypically distinct suppressor T cell lineage. Blood 2006;107: 4475–83.
37. Huttner KG, Breuer SK, Paul P, Majdic O, Heitger A, Felzmann T. Generation of potent anti-tumor immunity in mice by interleukin-12-secreting dendritic cells. Cancer Immunol Immunother 2005;54:67–77.
38. Wong RJ, Chan MK, Yu Z, et al. Angiogenesis inhibition by an oncolytic herpes virus expressing interleukin 12. Clin Cancer Res 2004;10:4509–16.
39. Hensbergen PJ, Wijnands PG, Schreurs MW, Scheper RJ, Willemze R, Tensen CP. The CXCR3 targeting chemokine CXCL11 has potent antitumor activity *in vivo* involving attraction of $CD8^+$ T lymphocytes but not inhibition of angiogenesis. J Immunother 2005;28:343–51.
40. Behrens GM, Li M, Davey GM, et al. Helper requirements for generation of effector CTL to islet β cell antigens. J Immunol 2004;172:5420–6.
41. Igawa T, Lin FF, Rao P, Lin MF. Suppression of LNCaP prostate cancer xenograft tumors by a prostate-specific protein tyrosine phosphatase, prostatic acid phosphatase. Prostate 2003;55:247–58.
42. Machlenkin A, Azriel-Rosenfeld R, Volovitz I, et al. Preventive and therapeutic vaccination with PAP-3, a novel human prostate cancer peptide, inhibits carcinoma development in HLA transgenic mice. Cancer Immunol Immunother. In press 2006.
43. Ciavarra RP, Holterman DA, Brown RR, et al. Prostate tumor microenvironment alters immune cells and prevents long-term survival in an orthotopic mouse model following flt3-ligand/CD40-ligand immunotherapy. J Immunother 2004;27:13–26.
44. Foster BA, Gingrich JR, Kwon ED, Madias C, Greenberg NM. Characterization of prostatic epithelial cell lines derived from transgenic adenocarcinoma of the mouse prostate (TRAMP) model. Cancer Res 1997; 57:3325–30.
45. Dzojic H, Loskog A, Totterman TH, Essand M. Adenovirus-mediated CD40 ligand therapy induces tumor cell apoptosis and systemic immunity in the TRAMP-C2 mouse prostate cancer model. Prostate 2006; 66:831–8.
46. Dyall R, Bowne WB, Weber LW, et al. Heteroclitic immunization induces tumor immunity. J Exp Med 1998; 188:1553–61.
47. Velders MP, McElhiney S, Cassetti MC, et al. Eradication of established tumors by vaccination with Venezuelan equine encephalitis virus replicon particles delivering human papillomavirus 16 E7 RNA. Cancer Res 2001;61:7861–7.
48. Perkins SD, O'Brien LM, Phillpotts RJ. Boosting with an adenovirus-based vaccine improves protective efficacy against Venezuelan equine encephalitis virus following DNA vaccination. Vaccine 2006;24:3440–5.
49. Pankewycz OG, Migliorini P, Madaio MP. Polyreactive autoantibodies are nephritogenic in murine lupus nephritis. J Immunol 1987;139:3287–94.
50. Wenderfer SE, Ke B, Hollmann TJ, Wetsel RA, Lan HY, Braun MC. C5a receptor deficiency attenuates T cell function and renal disease in MRL/lpr mice. J Am Soc Nephrol 2005;16:3572–82.